[1] Varun Krishna Paravasthu

[2] Balasubbareddy Mallala

[3] B.Mangu

Optimal Deployment of DGs, DSTATCOMs and EVCSs in Distribution System using Multi-Objective Artificial Hummingbird Optimization

JES
Journal of Electrical Systems

Abstract: - Distribution systems have a lot of obstacles to deal with, like increasing load demands, environmental issues, operating limits, and infrastructure development limitations. On the other hand, the number of plug-in hybrid electric vehicles (PHEVs) has grown significantly in recent years and is likely to continue due to concerns over the environment and fossil fuel shortages. Due to the increasing use of PHEVs, distribution systems were not built to accept them, requiring planners to create parking lots that support PHEV charging. To address these issues, in this study, optimal planning of distributed generation (DG) and electric vehicle charging stations (EVCS) in radial distribution systems by the maiden application of a novel Pareto-based multi-objective artificial hummingbird optimization (MOAHO) algorithm is addressed. Three technical aspects of the distribution system are improved by optimal planning of various types of DGs and EVCSs: active power loss reduction, total voltage deviation minimization, and voltage stability improvement. The Pareto-based MOAHO is employed to generate the optimal front between the three competing objectives and later TOPSIS method is employed for selecting the most compromised solution from the optimal front. The proposed methodology is tested on IEEE-33, IEEE-69 bus radial distribution test systems. To validate the efficacy of the MOAHO algorithm, the simulation outcomes of the proposed methodology are generated using a multi-objective non-dominated sorting genetic algorithm (NSGA2), particle swarm optimization algorithm (PSO), grey wolf optimization algorithm (GWO) and compared with the outcomes of the MOAHO algorithm.

Keywords: Multi-objective artificial hummingbird optimization (MOAHO) algorithm, Distributed Generation (DG), Electric vehicle charging station (EVCS), plug-in hybrid electric vehicles (PHEV), Distributed STATCOM (DSTACOM)

I. INTRODUCTION

The traditional power generation system comprises large-scale generation units and a wide interconnected transmission & distribution network that transmits and distributes electricity to household, commercial & industrial customers. Nowadays, transmission & distribution networks are under stress due to rising load needs, limited expansion choices, high I^2R losses in transmission & distribution networks, poor voltage profile, competitive power markets, depletion of fossil fuels and environmental issues. The increase in the usage of electric vehicles (EVs) would worsen the aforementioned issues. Therefore, to address the depletion of fossil fuel and environmental issues, renewable energy sources like Photo-Voltaic & Wind-Turbine units are highly integrated with the transmission networks & distribution networks.

Distributed generation units (DGs), which are alternatively referred to as decentralized generation, embedded generation, or dispersed generation, are generating units with few kW to 100's of MW that are either directly connected to the distribution network or installed at the metering site of the consumer. DG technologies include Photo-Voltaic (PV) units, Wind-Turbine (WT) units, Biomass units, Micro-Turbine, Fuel-cell, Battery energy storage system (BESS), Diesel generators, Synchronous condenser etc. DG technologies are grouped into four categories based on their capacity to support both active and reactive power. Fuel cells and microturbines are examples of Type-1 DGs that only support active power, whereas Synchronous compensators are examples of Type-2 DGs that only support reactive power. Real and reactive power are supported by Type-3 DGs, which include biomass generators based on synchronous generators, wind turbines (WT) with doubly fed induction generators, and photovoltaic (PV) systems with voltage source inverters. Wind turbines with induction generators are an example of Type-4 DGs that support both active and reactive power, but they consume reactive power. The

[1] *[1]Research Scholar, Dept. of Electrical Engineering, University College of Engineering, Osmania University, Hyderabad, varunkrishnaparavasthu@gmail.com

[2] Professor, Dept. of Electrical and Electronics Engineering, Chaitanya Bharathi Institute of Technology, Hyderabad

[3]Professor, Dept. of Electrical Engineering, University College of Engineering, Osmania University, Hyderabad

advantages like the requirement of small areas to install due to their compact size, technological advancements, less time for installation and the aforementioned issues associated with centralized generation have trigged the extensive usage of DGs in transmission & power distribution networks, and nearby load centres. And, Improvements in technical metrics like I^2R loss reduction, voltage profile, reliability, voltage stability, loadability are attained due to the connection of DGs in the distribution system. However improper placement of DGs with improper size in the distribution system could have worsened the technical metrics instead of improving them. Therefore, finding the optimal number, optimal location, and optimal size of DGs in the distribution system is coined as the optimal planning of DGs (OPDG) problem.

In [1]–[4], the authors presented a detailed review of the OPDG problem in the distribution system using several analytical techniques, and meta-heuristic optimization algorithms. The authors of [5] introduced an analytical method that utilizes an exact loss formula to determine the most effective capacity and placement of a distributed generator (DG) while reducing power losses in the system. However, it was limited to a single DG unit allocation and required bus impedance matrix calculation, resulting in computation inefficiencies in large-scale distribution networks. The authors improved an earlier method [5] to develop analytical expressions for optimal DG placement in [6], which was confined to units with active power generation. The research presented in [7] used analytical formulas based on [6] to calculate the optimal size, location, and power factor for dispatchable and non-dispatchable DGs, taking into account demand and renewable generation uncertainty. The authors of [8] suggested a multi-objective index-based analytical method to calculate the appropriate capacity of PV-based DG units. An analytical technique based on the branch current formula was devised in [9] to minimize loss for allocating numerous DG units. An equivalent current injection method was described in [10] to identify the ideal DG size and position while minimizing power losses. Most research focuses on optimizing DG planning using analytical techniques for power loss mitigation and voltage profile improvement.

PSO is used to solve optimal DG deployment problem in distribution systems with changing power loads and non-unity power factors [11]. An enhanced PSO is suggested for optimal placement of DGs that inject real power and/or absorb reactive power [12]. To minimize power loss, firefly and backtracking search algorithms are used to optimize multi-DG unit planning, including determining optimal DG locations, sizes, and power factors [13]. In [14], authors used UVDA-based heuristics to optimize Type-3 DG allocation and power factor to reduce network active power loss. The HPSO method was used to optimize the system's maximum loadability [15]. In [16], the authors employed a hybrid genetic dragonfly optimization technique to minimize the distribution system's EENS reliability index by optimizing DG sizes and locations. The authors of [17] used the Harmony search optimization algorithm (HSA) to minimize network power loss, and total harmonic distortion, improve system voltage profile, and enhance security. The authors of [18] employed a TLBO-GWO optimization technique to allocate Type-1 and Type-3 DGs with optimal power factors to the distribution network to lower I^2R loss and boost reliability. In [19], authors explored a weighted-based hybrid SFLA and DE algorithm for optimal placement of DGs in distribution systems for reducing power loss, operational expenses, and emission costs. To minimize active power loss, improve the voltage profile, and strengthen the voltage stability of the system, the authors in [20] used a weighted factor multi-objective approach to solve the OPDG problem. In [21] , multi-objective Max-Min & epsilon approach are put out to reduce I^2R loss and maximize network loadability. Pareto-based Harris hawk optimization is used in [22] to enhance system technical parameters.

Concerns surrounding the exhaustion of fossil fuels, CO2 emissions, and the greenhouse effect have led to a trend towards emissions-free plug-in battery-fuelled electric vehicles (PHEVs), which are expected to play a key part in the road transportation system. A comprehensive review of electric vehicle technologies and the effect of plug-in hybrid electric vehicle demand on load profile may be found in [23], [24]. Numerous researchers have concentrated on DG planning in distribution systems to mitigate the effects of PHEV load demand and to improve system performance. The authors [25] used the HPSO-GWO algorithm to determine the optimal location for EVCS and RDGs in the distribution system. A study on EVCS placement aims to minimize power loss and maximize distribution system stability, using APSO is discussed in [26]. In, [27] the fuzzy-based multi-objective grasshopper optimization method is used for RDG and EVCS optimal planning to improve the distribution system's technical metrics. The optimum approach to integrate RDG, EVCS, and BESS to enhance the technical distribution systems was investigated by authors in [28] using a Pareto-based WOAGA algorithm. In [29-35] authors proposed different single and multi-optimization algorithms to minimize different power system optimization parameters.

From the literature review, it is evident that various types of DGs are rarely explored in existing literature. This study encompasses diverse DG technologies in conjunction with the simultaneous planning of EVCS Furthermore, the majority of studies utilize single-objective optimization algorithms such as PSO, GWO, DE, SLFA and TLBO to address the DG deployment problem. However, these single-objective optimizers lack the capability to handle multiple objectives concurrently. Consequently, authors frequently resort to employing a weighted-sum approach [43] to transform the multi-objective problem into a single-objective one. Despite its simplicity in implementation, this approach suffers from the drawback that decision-making precedes the optimization process, potentially leading to suboptimal solutions that may not align with the conflicting objective preferences of decision-makers [44]. To mitigate these limitations, this study adopts a Pareto-based multi-objective AHO (MOAHO) algorithm, which can optimize multiple objectives simultaneously. The MOAHO algorithm generates a set of solutions known as Pareto optimal solutions. The technique for order of preference by similarity to ideal solution (TOPSIS) is then employed to identify the most compromised solution from the Pareto optimal solution frontier. The contributions of this study are outlined as follows:

1) Presenting a comprehensive approach that simultaneously plans DGs and EVCS, considering diverse DG types and operating power factors.

2) Adopting the Pareto-based MOAHO to minimize real power loss, total voltage deviation and voltage stability index is improved in distribution systems. This algorithm facilitates the simultaneous optimal planning of multiple DG technologies and EVCSs.

3) Utilizing TOPSIS to select the most balanced solution from the Pareto front generated by the MOAHO algorithm. Moreover, exploring TOPSIS capabilities to suggest solutions accommodating diverse decision-makers objective preferences.

4) Conducting a comparative analysis between the MOAHO algorithm and established algorithms such as NSGA-II, MOPSO, and MOGWO. This analysis encompasses standard IEEE-33 bus, IEEE-69 bus systems, incorporating various scenarios and cases for comprehensive evaluation.

The remaining part of the article is articulated as follows, Section 2 discusses the objective functions and operating constraints. Section 3 presents the AHO algorithm, Pareto-based MOAHO algorithm, TOPSIS method and detailed implementation aspects of the algorithm. The proposed methodology and simulation outcomes are discussed in section 4 and the conclusion & future aspects of the work are given in section 5.

II. PROBLEM FORMULATION

This section presents the modelling of DGs, DSTACOMs & EVCSs, objective functions and operating constraints associated with the efficient planning of DGs and EVCSs in radial distribution networks.

A. Modelling of DGs and EVCSs

Figure1 depicts the simple distribution with DGs, DSTACOMs and EVCSs. The introduction of DGs, DSTATCOMs and EVCSs turns the passive radial distribution system into an active one due to bidirectional flows in the system.
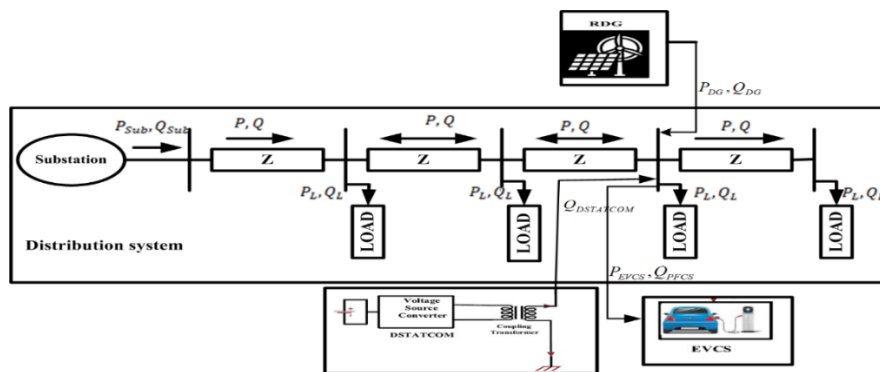
Figure 1 simple distribution system with DGs, DSTATCOMS and EVCSs

For load flow analysis, DGs are modelled using a negative PQ type of load model. About the above-cited method, the net power demand at the bus in the distribution system is the difference of conventional load demand & DG power. The power due to EVCSs will aid the conventional load demand. Therefore, the net load demand for a bus in the distribution system is given by

$$P_{n,net} = P_{n,L} + P_{EVCS} - P_{DG}$$

(1)

$$Q_{n,net} = Q_{n,L} + Q_{EVCS} - Q_{DG} - Q_{DSTATCOM}$$

(2)

B. Objective Functions

In this study, the enhancement of three technical metrics of the distribution system by optimal planning of DGs and EVCSs is considered. The mathematical formulations of the metrics are given below.

1 Real Power loss

The real power loss (RP_{loss}) of the distribution system ought to be reduced as much as possible to improve the efficiency of the distribution system.

$$F_1 = minimize \ (RP_{loss})$$

(3)

$$RP_{loss} = \sum_{k=1}^{nobr} I_k^2 * R_k$$

(4)

Where, I_k is the kth branch current, R_k is the resistance of the kth branch and nobr represents the total number of branches

2 Total Voltage Deviation

To maintain the bus voltages of the distribution system as much as close to the reference value, Total Voltage Deviation (TVD) of the system has to be minimized

$$F_2 = minimize \ (TVD)$$

(5)

$$TVD = \sum_{n=1}^{nobus}(|1 - V_n|)^2$$

(6)

Where, V_n is the nth bus voltage and $nobus$ represents the total number of buses.

3 Voltage Stability Index

Voltage stability of the system should be maximized to maintain the overall stability of the system [38].

$$F_3 = maximize \ (VSI)$$

(7)

$$vsi_n = V_n^4 - 4 \ (P_n R_{mn} - Q_n X_{mn})^2 - 4 \ V_n^2(P_n X_{mn} + Q_n R_{mn})$$

(8)

$$VSI = min \ (vsi_n)$$

(9)

C. Operating Constraint's

The optimal planning of DGs and EVCSs problem in distribution systems are subjected to the following operational constraints

1 The magnitude of the voltage on each bus ought to fall between the bounds of the lowest and maximum values.

$$|V_{min}| < |V_n| < |V_{max}| \qquad n = 1,2 \dots \dots nobus \qquad (10)$$

2 The current via each branch should be less than its rating.

$$I_k \leq I_k^{max} \qquad\qquad k = 1,2 \dots \dots nobr$$

(11)

3 Real and reactive power injected by DGs ($P_{j,DG}$) ought to fall between the bounds of the lowest and maximum values.

$$P_{j,DG}^{min}, Q_{j,DG}^{min} \leq P_{j,DG}, Q_{j,DG} \leq P_{j,DG}^{max}, Q_{j,DG}^{max} \qquad j = 1,.,3,\dots.nodg$$

(12)

where, *nodg* is the total number of DGs connected in the distribution system.

4   Operating power factor of DGs ought to fall between minimum (pf_j^{min}) and unity power factor limits.

$$pf_j^{min} \leq pf_j \leq 1$$

(13)

Total real power ($P_{Tot,DG}$) and reactive power generated ($Q_{Tot,DG}$) by DGs should be less than the real active and reactive power load of the system (both conventional & EVCSs load demands) respectively.

$$\sum_{j=1}^{nodg} P_{j,DG} = P_{Tot,DG} \leq P_{cload} + P_{EVCS} \qquad (14)$$

$$\sum_{j=1}^{nodg} Q_{j,DG} = Q_{Tot,DG} \leq Q_{cload} + Q_{EVCS}$$

(15)

5   Real Power and Reactive power balance constraints.

$$P_{slack} + P_{Tot,DG} = P_{cload} + P_{EVCS} + P_{loss}$$

(16)

$$Q_{slack} + Q_{Tot,DG} = P_{cload} + P_{EVCS} + Q_{loss}$$

(17)

III.   OPTIMIZATION ALGORITHM

A Artificial Humming bird optimization (AHO) algorithm

AHO is an optimization method developed based on bioinspired metaheuristics [39]. This algorithm is inspired by the social behaviour of hummingbirds, including their clever foraging strategies and extraordinary flying abilities. In basic terms, AHO mimics directed foraging, territorial foraging, and migrating foraging in addition to three distinct search strategies, including omnidirectional, axial, and diagonal flights.

The Pseudo Code of the overall general architecture of AHO is depicted in Figure 2

Initialization

While the criteria for discontinuing is not met

Guided foraging

Migrating foraging and

territorial foraging

End
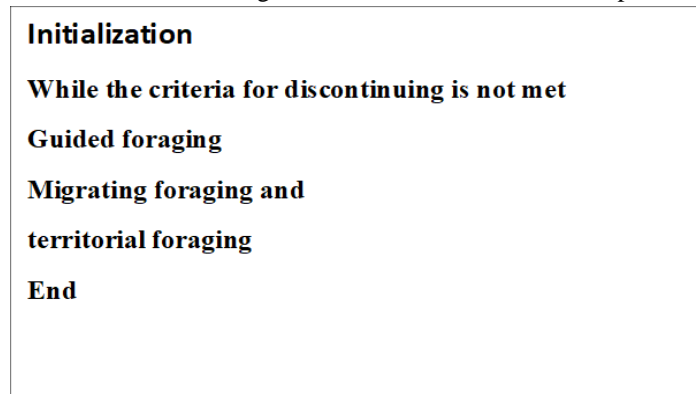
Figure 2 Pseudo Code of the overall general architecture of AHO

The mathematical equations for position update equations of AHO during each are given below.

B Initialization

The first set of solutions between the minimum and maximum boundary values are generated in this step.

$$x_i^j = LB_i^j + \left(UB_i^j - LB_i^j\right) * rand \quad i = 1\dots N, j = 1\dots.dim$$

(18)

where x_i^j represents the jth dimension of ith agent or hummingbirds, N represents the number of agents, dim represents the dimension.

Apart from the initialization of the initial set of solutions, a visit table is formed in this step.

$$VT_i^j = \begin{cases} 0 \ if \ i \neq j \\ null \ if \ i = j \end{cases}$$

(19)

C Guided foraging

The following represents the mathematical equations for incorporating the guided foraging behaviour for updating hummingbird position towards potential or global food sources as follows

$$v_i^{dim}(t+1) = x_{tar}^{dim}(t) + \text{rand} * D * \left(x_i^{dim}(t) - x_{tar}^{dim}(t)\right)$$

(20)

Where $x_{tar}^{dim}(t)$ represents the position of the target/potential/global best food force, rand is the random number between 0 & 1, D represents the introduction of axial flight [39] searching pattern during the direct foraging search phase.

$$x_i(t+1) = \begin{cases} v_i(t+1) \ if \ f(v_i(t+1) < fx_i(t)) \\ x_i(t) \ if \ f(v_i(t+1) > f \ x_i(t)) \end{cases}$$

(21)

D Territorial foraging

To find an additional source of food, the hummingbird can thus travel to the adjacent area inside its domain. The local food search and territorial foraging strategy's mathematical expressions are given below

$$x_i(t+1) = x_i(t) + rand * D * x_i(t)$$

(22)

E Migrating foraging

When the hummingbirds' normal food source isn't available in their area, they move to areas with more food sources. The mathematical equation for a hummingbird's migrating foraging travel is given below

$$x_i^j(t+1) = LB_i^j + \left(UB_i^j - LB_i^j\right) * rand \ i = 1 \dots N, j = 1 \dots \dots dim$$

(23)

The comprehensive pseudocode for the AHO optimization method can be found in [39]

F Pareto-based MOAHO

A Pareto-based multi-objective technique [40] is an optimization strategy that is based on Pareto optimality and seeks to manage several competing objectives at once. The primary characteristic of Pareto-based techniques is their capacity to produce a collection of solutions, as opposed to a single ideal one, that show trade-offs between conflicting goals. This technique aims to identify solutions that are not superior (or) dominated to any other solution across all the objectives that are taken into consideration. These non-dominated solutions collectively form the Pareto front, representing the optimal trade-offs among conflicting objectives. This multi-objective technique can be expressed mathematically as

solution-p (sol_p) dominates solution-q (sol_q), if the following condition is met

$$\forall n \in \{1,..3,\dots, \text{nobj}\} \rightarrow F_n(sol_p) \leq F_n(sol_q)$$

(24)

$$\wedge \exists n \in \{1,\dots 3,\dots, \text{nobj}\} \rightarrow F_n(sol_p) < F_n(sol_q)$$

(25)

where $F_n(sol_p)$ represents the nth objective function value of solution q.

In this way, If the solution sol_m dominates all the solutions, sol_m enters into a non-dominant solution set

G Crowding distance metric

The crowding distance metric (C_r) is computed for each solution in the Pareto front to restrict the total number of solutions to a predetermined number, say. The solutions with the highest C_r are then kept in a collection known as the repository. The crowding distance metric for the nth solution (C_{rn}) in the Pareto front is expressed mathematically as

$$(C_{rn}) = \sum_{k=1}^{nobjec} \frac{F_k^{n+1} - F_k^{n-1}}{F_k^{max} - F_k^{min}}$$

(26)

H TOPSIS method

A decision-making process called the Technique for Order of Preference by Similarity to Ideal Solution (TOPSIS) is intended to help choose the best option out of a given set of non-dominated solutions. Based on how close each solution in the non-dominated set to the positive ideal solution (PIS) and the negative ideal solution (NIS), this technique evaluates each solution. The TOPSIS approach is described in the following steps [44]:

1) Formulation of a decision matrix (X) with the rows of m alternatives and the columns of n objectives.

$$X = \begin{bmatrix} F_1^1 & F_1^2 & \ldots\ldots\ldots\ldots F_1^n \\ F_2^1 & F_2^2 & \ldots\ldots\ldots\ldots F_2^n \\ & & \cdot \\ & & \cdot \\ F_m^1 & F_m^2 & \ldots\ldots\ldots\ldots F_m^n \end{bmatrix} \tag{27}$$

2) Formulation of normalized decision matrix (NX).

$$NX = \begin{bmatrix} nF_1^1 & nF_1^2 \ldots\ldots\ldots\ldots nF_1^n \\ nF_2^1 & nF_2^2 \ldots\ldots\ldots\ldots nF_2^n \\ & \cdot \\ & \cdot \\ nF_m^1 & nF_m^2 \ldots\ldots\ldots\ldots nF_m^n \end{bmatrix} \qquad \text{where } nF_m^n = \frac{F_m^n}{\sqrt{\sum_{i=1}^m F_m^i}}$$

(28)

3) Formulation of normalized decision matrix (WNX).

$$WNX = \begin{bmatrix} wnF_1^1 & wnF_1^2 \ldots\ldots\ldots\ldots wnF_1^n \\ wnF_2^1 & wnF_2^2 \ldots\ldots\ldots\ldots wnF_2^n \\ & \cdot \\ & \cdot \\ wnF_m^1 & wnF_m^2 \ldots\ldots\ldots\ldots wnF_m^n \end{bmatrix} \tag{29}$$

where $wnF_m^n = (w_1 * nF_m^1 + w_{2*}nF_m^2 + \ldots\ldots\ldots + w_{n*}nF_m^n)$, w_n is the weight assigned to objective function.

4) Determination of positive & negative ideal solution (PIS & NIS).

$$PIS = \{pi_1^+ \quad pi_2^+ \ldots\ldots\ldots pi_n^+\}$$
$$NIS = \{ni_1^- \quad ni_2^- \ldots\ldots\ldots ni_n^-\} \tag{30}$$

$$\text{where } \begin{array}{l} pi_n^+ = min\{wnF_1^n \quad wnF_2^n \ldots\ldots\ldots wnF_m^n\} \\ ni_n^- = max\{wnF_1^n \quad wnF_2^n \ldots\ldots\ldots wnF_m^n\} \end{array}$$

(31)

5) Calculation of Euclidian distance from PIS & NIS.

$$ed_i^+ = \sqrt{\left(\sum_{j=1}^n wnF_i^j - pi_j^+\right)^2} \quad i = 1\ldots m \tag{32}$$

$$ed_i^- = \sqrt{\left(\sum_{j=1}^n wnF_i^j - ni_j^-\right)^2} \quad i = 1\ldots m \tag{33}$$

6) Relative closeness index (RCI_i) of each solution is determined.

$$RCI_i = \frac{d_i^-}{d_i^- + d_i^+} \quad i = 1\ldots m \tag{34}$$

7) The alternative with the highest RCI_i is considered as the best choice according to the TOPSIS method

I Implementation of TOPSIS-MOAHO algorithm

The following outlines the step-by-step process for the TOPIS-MOAHO algorithm for finding the optimal location sizes of DGs & EVCSs for enhancing above cited objectives

1. Read the line and load information from the distribution system
2. Initialising the algorithm's parameters, like the number of agents (N), the maximum number of iterations (Maxiter), the size of the Archive, and so on

3.   Generation of initial set of hummingbird positions between minimum and maximum decision variable boundary limits

4.   For every search agent, do power flow analyses to determine the objective function values

5.   Finding of non-dominated solutions using the concept addressed in section 3.2 and update the solutions in the archive set using the concept addressed in section 3.3

6.   Set iteration count t =0

7.   Update the humming bird's positions using the methodology discussed in Section 3.1

8.   Calculate updated humming bird agent's objective function values by performing load flow analysis

9.   Merge new hummingbird agents and old hummingbird agents positions and find the non-dominated solutions using the concepts discussed in section 3.2 and update the positions in the archive set using the concept discussed in section 3.3

10.   Repeat steps 6-9 until current iteration fall below the maximum iteration number, otherwise print the final outcomes: the most compromised solution using the TOPSIS methodology addressed in section 3.4

The flowchart of the TOPIS-MOAHO technique for optimal deployment of DGs and EVCSs is depicted in Figure 3
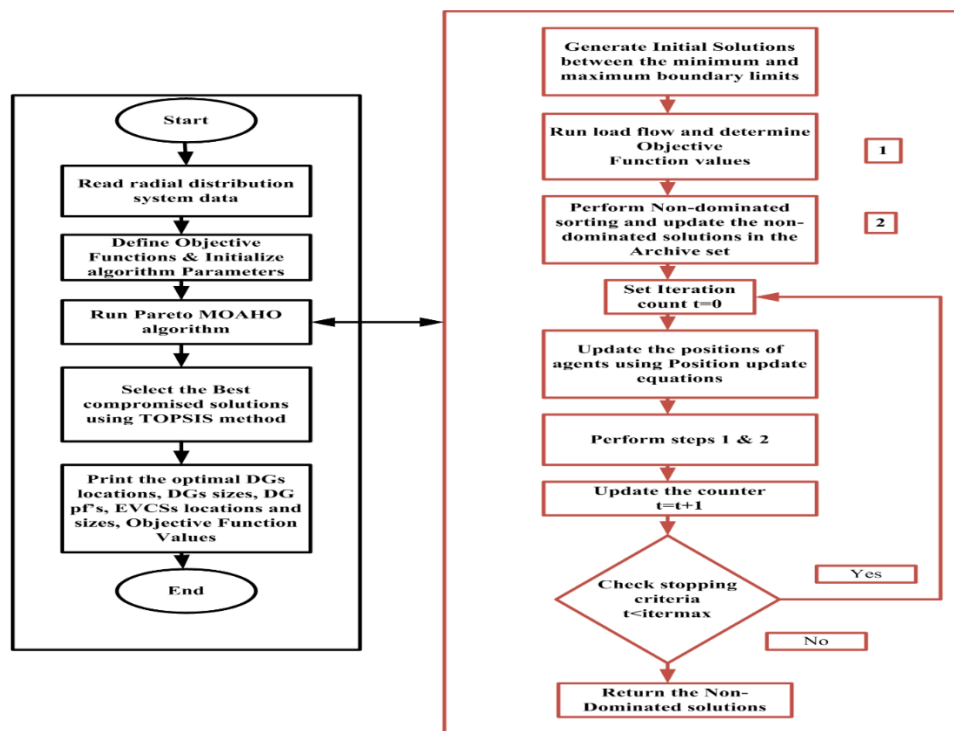
Figure 3 Flowchart of TOPIS-MOAHO technique for optimal
deployment of DGs and EVCSs in the distribution system

IV.   RESULTS AND DISCUSSIONS

In this section, the impact on the improvement of three distribution system metrics (network power loss minimization, minimization of total voltage deviation and maximization of voltage stability index) due to optimal deployment of various DG technologies is presented at first. Then the enhancement of the above-cited metrics by simultaneous optimal deployment of DGs and EVCSs is discussed in the second stage. The following cases are considered in this work

Case-0: Without DGs and EVCSs

Case-1: Optimal Planning of DGs operating with upf (Type-1 DGs)

Case-2: Optimal Planning of DGs operating with upf and zpf (Type-1 & Type-2 DGs)

Case-3: Optimal Planning of DGs operating with 0.9 pf (Type-3 DGs)

Case-4: Optimal Planning of DGs operating with optimal pf (Type-3 DGs)

Case-5: Optimal Planning of DGs operating with 0.9 pf followed by Optimal Planning of EVCSs

Case-6: Simultaneous Optimal Planning of DGs with upf & zpf and EVCSs

Case-7: Simultaneous Optimal Planning of DGs with 0.9 pf and EVCSs

Case-8: Simultaneous Optimal Planning of DGs with optimal pf and EVCSs

where pf, upf and zpf refer to the power factor, unity power factor and zero power factor. Cases 1-4 deal with the optimal deployment of different DG technologies, case 5 deals with the optimal planning of EVCSs after the optimal planning of DGs, and cases 6-8 deal with the simultaneous optimal deployment of DGs and EVCS. Three standard IEEE-33,69 bus systems comprised of small, medium and large-scale radial distribution systems are considered. A Pareto-based novel multi-objective hummingbird optimization algorithm (MOAHO) has been employed for generating the optimal Pareto fronts between the conflicting objectives. TOPSIS method is employed for selecting the most (or) best compromised solution from the optimal pareto front. In step 3 of the TOPSIS method, the weights related to objectives F_1 $(Power\ loss), F_2(TVD), F_3(VSI)$ are coined as w_p, w_{vd}, w_{vs}. The outcomes of the TOPSIS-MOAHO algorithm are compared with MOPSO, MOGWO & NSGA-II algorithms. The proposed optimal deployment problem of DGs and EVCSs using TOPSIS-MOAHA, MOPSO, MOGWO & NSGA2 is developed under the MATLAB environment and was executed on a personal computer having Intel(R) Core (TM) i5-7200U CPU @ 2.50GHz processor with installed RAM of 8 GB. Population size of 300, Archive size of 200 and maximum number of iterations of 600 are considered for all algorithms. The remaining control parameters of all algorithms were initialized to the values quoted in [41].

A. *IEEE-33 BUS SYSTEM*

The single-line diagram of the 33-bus radial distribution system is depicted in Figure 4. A detailed description of the 33-bus system can be found in [42]. The total real and reactive power demands of the system are 3715 kW and 2300 kVar. The base MVA and kV are 100 and 12.66. In case-0, load flow analysis for the initial assessment of the system without DGs and EVCSs is performed. Load flow results indicate a real power loss of 210.98 kW, TVD of 0.1338 p.u and VSI of 0.6672 p.u.
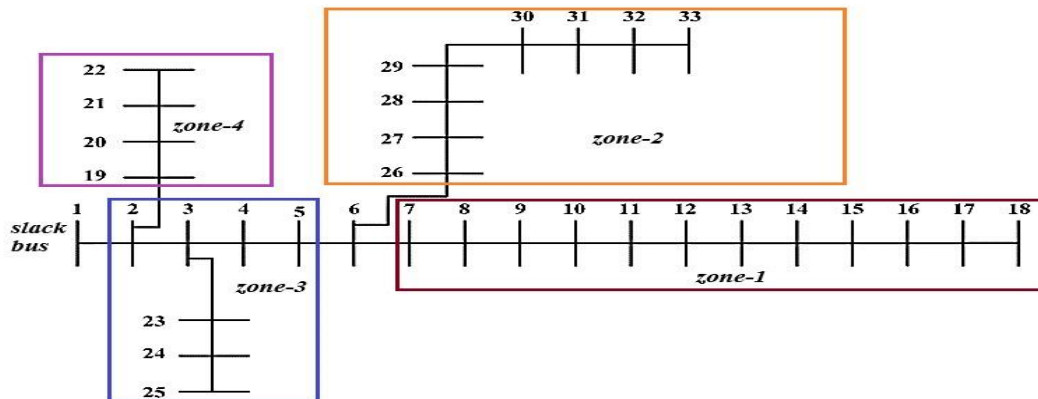
Figure 4 Single diagram of 33 bus system

B. *DGs deployment*

Optimal Pareto fronts generated by MOAHA, MOPSO, MOGWO and NSGA-II algorithms for cases 1-4 of the 33-bus system are depicted in Figure 5.
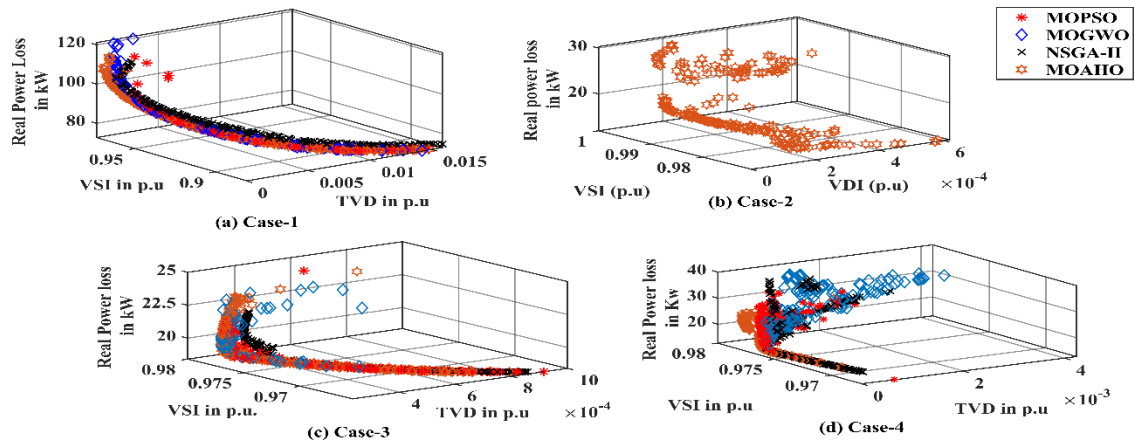
Figure 5 Optimal Pareto fronts of MOAHA, MOPSO, MOGWO & NSGA-II
algorithms for cases 1-4 of the 33-bus system

The outcomes like DGs locations, DGs sizes, DGs pf, and system technical parameters for cases 1-4 generated by the TOPSIS-MOAHO algorithm (with equal weightage (w_p, w_{vd}, w_{vs})=1/3) are tabulated in Table 1. From the outcomes tabulated in Table 1 for cases 1-4, the following observations are made. In case-1, due to the connection of DGs operating with upf at optimal locations 13, 24, 30 with optimal capacities of 1155 kW, 1071 kW, and 1572 kW respectively, system power loss reduced to 91.023 kW accounts for 56.85 % loss reduction, TVD is reduced to 0.0012 p.u and VSI is maximized to 0.9595 p.u In case-2, system power loss reduced to 17.181 kW accounts for 91.860 % loss reduction, TVD is reduced to 0.00005 p.u and VSI is maximized to 0.9881 p.u due to the optimal connection of Type-1 & Type-2 DGs in the system. In case-3, loss is mitigated to 19.183 kW, TVD is reduced to 0.00023 p.u and VSI is maximized to 0.9768 p.u due to optimal planning of Type-3 DGs operating with 0.9 pf and in case-4, loss is mitigated to 13.342 kW, TVD is mitigated to 0.00024 p.u and VSI is maximized to 0.9766 p.u due to optimal connection of Type-3 DGs operating with optimal pf. The outmost improvement in TVD & VSI of the system is observed during optimal deployment of Type-1 & Type-2 DGs, balanced improvement in three technical metrics is of the system is observed in case-4 i.e., due to optimal deployment of Type-3 DGs operating with optimal pf.

Table 1 Results of 33 bus system for cases 0-4

Case No	DG loc's/DG Sizes (KW/KVAR) /DG's pf	RP_{loss} in KW	TVD in p.u	VSI in p.u	% RP_{loss} reduction	Minimum Voltage in p.u
0	---------	210.98	0.1338	0.6672	----------	0.9038
1	13/1155/1,24/1071/1 30/1572/1	91.023	0.0012	0.9595	56.857	0.9895
2	14/0827/1,24/1355/1 30/1055/1,08/0689/0 21/0272/0,30/0972/0	17.181	0.00005	0.9881	91.860	0.997
3	13/0837/0.9, 24/1177/0.9 30/1350/0.9	19.183	0.00023	0.9768	90.907	0.9942
4	**13/0810/0.88,24/1119/0.88 30/1206/0.80**	**13.342**	**0.00024**	**0.9766**	**93.679**	**0.9942**

Several weight combinations are chosen for investigation in order to examine the effects of weight allocations to stage III of TOPSIS objectives. The findings were then carefully examined. Table 2 depicts the impact on the technical metrics improvement during the optimal deployment of DGs in cases 1-4 due to the consideration of different weights during the selection of compromised solutions using the TOPSIS method.

Table 2 Results of cases 1-4 of 33 bus system for different weights

Case No	Weights	DG loc's/DG Sizes (KW/kVAR) /DG's pf	RP_{loss} in kW	TVD in p.u	VSI in p.u
1	w_p, w_{vd}, w_{vs} (1,0,0)	13/807/1,24/1080/1,30/1054/1	72.786	0.0149	0.8817
	w_p, w_{vd}, w_{vs} (0,1,0)	14/1087/1,29/2145/1,25/0589/1	114.3081	0.0004	0.9696
	w_p, w_{vd}, w_{vs} (0,0,1)	13/1311/1,25/781/1,30/1727/1	107.2547	0.0006	0.9738
	w_p, w_{vd}, w_{vs} (1/2,1/2,0)	13/1154/1,24/1071/,30/1572/1	92.365	0.0013	0.9596
2	w_p, w_{vd}, w_{vs} (1,0,0)	24/1089/1,14/764/1,30/1016/1,11/468/0 30/0974/0,24/0487/0	11.962	0.0006	0.9715
	w_p, w_{vd}, w_{vs} (0,1,0)	25/1223/1,15/782/1,30/1349/1,08/682/0 28/0799/0,21/0387/0	29.813	0.00005	0.9927
	w_p, w_{vd}, w_{vs} (0,0,1)	25/1202/1,15/817/1,30/1403/1,08/637/0 28/0973/0,21/0406/0	23.232	0.0006	0.9972
	w_p, w_{vd}, w_{vs} (1/2,1/2,0)	24/1355/1,14/827/1,30/1055/1 08/689/0,30/0973/0,21/0272/0	17.18	0.00009	0.9881
3	w_p, w_{vd}, w_{vs} (1,0,0)	13/795/0.9,24/1074/0.9,30/1235/0.9	18.40	0.0008	0.9664
	w_p, w_{vd}, w_{vs} (0,1,0)	13/830/0.9,24/12205/0.9,30/1363/0.9	19.814	0.0002	0.977
	w_p, w_{vd}, w_{vs} (0,0,1)	12/1068/0.9,24/1389/0.9,30/1280/0.9	23.93	0.0008	0.9779
	w_p, w_{vd}, w_{vs} (1/2,1/2,0)	13/0817/0.9,24/1084/0.9,30/1254/0.9	18.484	0.0005	0.971
4	w_p, w_{vd}, w_{vs} (1,0,0)	14/0766/0.88,24/1047/0.87 30/1105/0.80	12.885	0.00063	0.9672
	w_p, w_{vd}, w_{vs} (0,1,0)	13/0750/0.84,24/0971/0.83 29/1351/0.83	17.043	0.00023	0.9768
	w_p, w_{vd}, w_{vs} (0,0,1)	13/0872/0.80,24/1584/0.80 29/1186/0.80	28.773	0.0022	0.9787
	w_p, w_{vd}, w_{vs} (1/2,1/2,0)	13/0787/0.86,24/1052/0.89 30/1204/0.81	13.350	0.00027	0.9763

From the outcomes tabulated in Table 2, it is observed that power loss is mitigated to the utmost value for weights $w_p, w_{vd}, w_{vs} = (1,0,0)$, TVD is reduced to the utmost value for weights $w_p, w_{vd}, w_{vs} = (0,1,0)$, VSI is enhanced to the utmost value for weights $w_p, w_{vd}, w_{vs} = (0,0,1)$ and balanced improvement in all metrics is observed for weights $w_p, w_{vd}, w_{vs} = (1/3,1/3,1/3)$. Due to the consideration of TVD & VSI as one of the objective functions, the better improvement in TVD & VSI in respective cases is achieved by drawing more power from DGs into the system. Depending on the importance given to improvement in technical metrics, the distribution operator (or) planner may choose one solution from the solutions tabulated in Table 2.Figure 6 depicts the 33-bus system voltage profile box plot of cases 1-4 for different weights. It can be seen from Figure 6 that whenever TVD is considered as one of the target functions, the system's bus voltages are significantly closer to reference values.
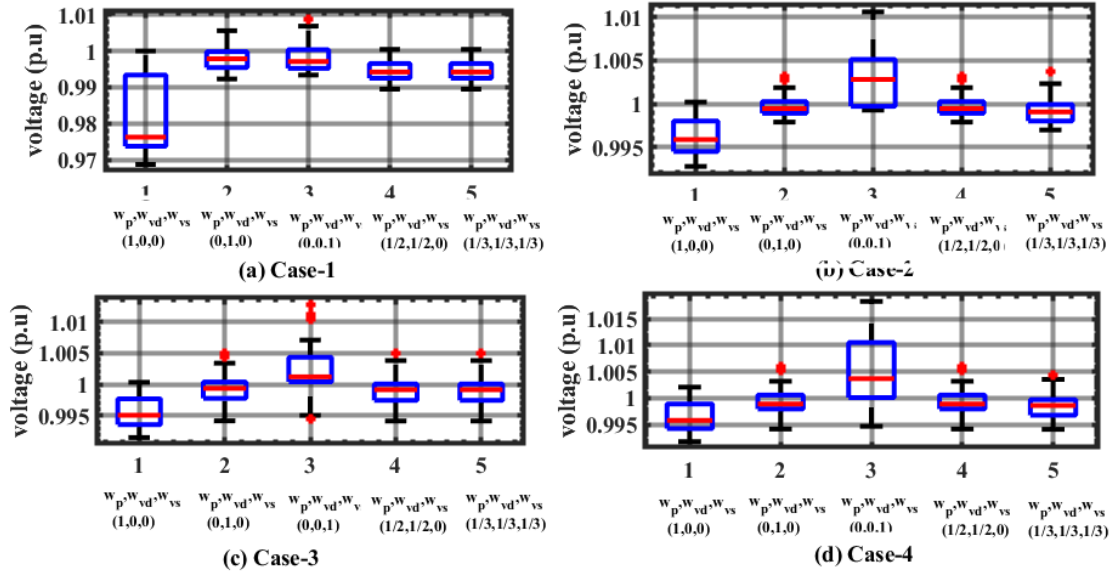
Figure 6 33-bus system voltage profile box plot of cases 1-4 for different weights

C.   Simultaneous DGs & EVCSs deployment

Based on the survey reported in [43], the optimal planning of one charging station in each zone depicted in Figure. 4 with a total of four charging stations having a total charging station capacity of 800 kVA are considered in the 33-bus system. Optimal Pareto fronts generated by MOAHA, MOPSO, MOGWO and NSGA-II algorithms for cases 5-8 of the 33-bus system are depicted

in Figure 7.
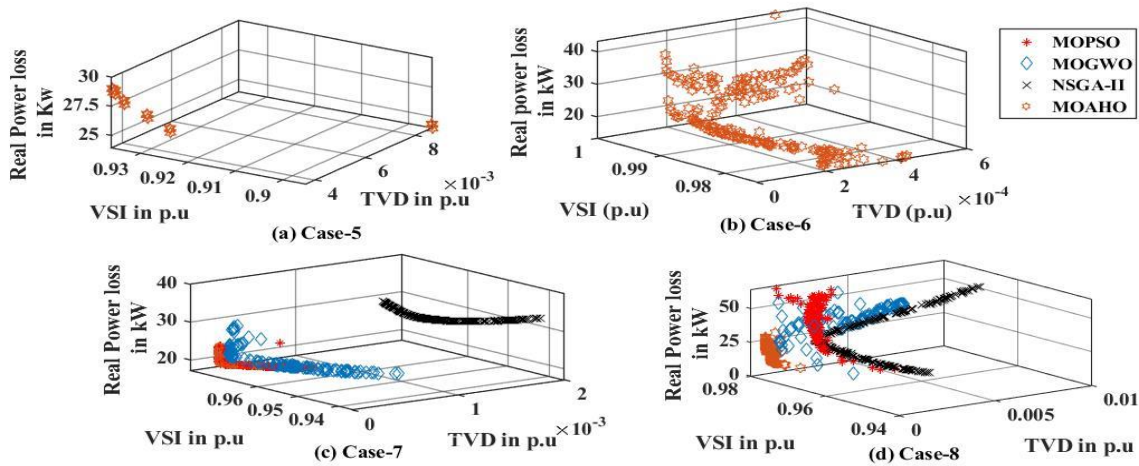
Figure 7 Optimal Pareto fronts of MOAHA, MOPSO, MOGWO & NSGA-II algorithms for cases 5-8 of the 33-bus system

The outcomes like DGs locations, DGs sizes, DGs pf, EVCSs locations, EVCSs sizes, and system technical parameters for cases 5-8 were generated using the TOPSIS-MOAHO algorithm (with equal weightage (w_p, w_{vd}, w_{vs})=1/3) are tabulated in Table 3.

Table 3 Results of 33 bus system for cases 5-8

Case No	DG loc's/DG Sizes(KW/KVAR) /DG's pf	EVCS loc/EVCS Sizes (kVA)	RP_{loss} in KW	TVD in p.u	VSI in p.u	% RP_{loss} reduction	Minimum Voltage in p.u
5	13/0835/0.9 24/1076/0.9 30/1356/0.9	07/300,27/300 24/150,19/150	28.411	0.0037	0.9359	86.533	0.9836
6	14/1129/1 24/1517/1 29/1455/1 09/0676/0 21/0326/0 30/1109/0	14/300,29/300 24/150,19/150	20.2506	0.0001	0.9875	90.40	0.9969
7	13/1115/0.9 24/1345/0.9 30/1620/0.9	13/300,30/300 24/150,19/150	18.142	0.00024	0.9756	91.401	0.9939
8	13/1126/0.91 24/1399/0.91 30/1433/0.80	13/300,30/300 24/150,19/150	13.193	0.00025	0.9756	93.746	0.9939

In case-5, optimal planning of DGs operating with 0.9 pf followed by optimal planning of EVCSs is addressed. From the outcomes, it was observed that technical parameters are worsened in case 5 in comparison to the metrics quoted in case 4 due to the additional EVCS load on the system. Simultaneous optimal planning of EVCSs and DGs is addressed in cases 6-8. The utmost improvement in three technical metrics is observed in case-8 during simultaneous optimal planning of EVCSs and DGs operating with optimal pf i.e., power loss is reduced to 93.74%, TVD is mitigated to 0.00025, VSI is maximized to 0.9756. Figure 8 depicts the voltage profile of the system for all the cases 0-8. From Figure 8, it was observed that the voltage profile of the system is improved in all the cases and all the bus voltage limits are within minimum and maximum voltage permissible limits
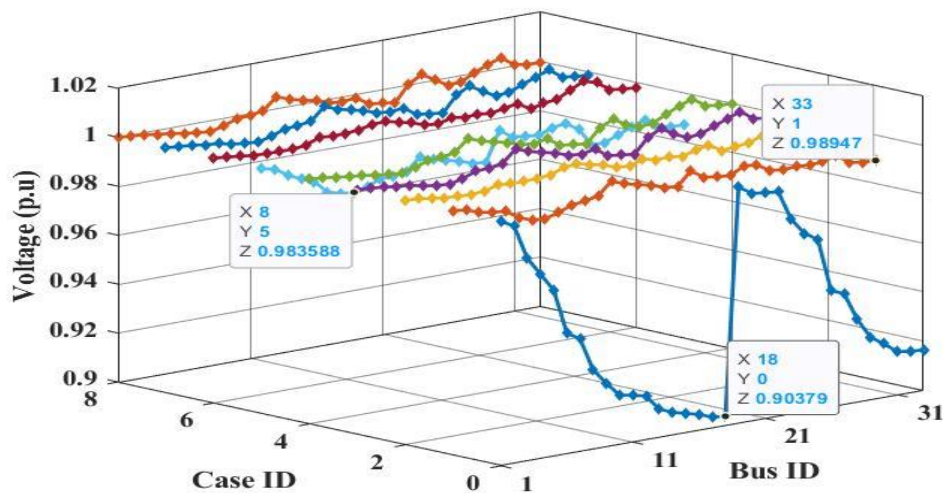
Figure 8 Voltage profile of 33 bus system for the outcomes of TOPSIS-MOAHO with equal weightage generated in different cases

Table 4 depicts the impact on the technical metrics improvement during the optimal deployment of DGs in case 8 due to the consideration of different weights during the selection of compromised solutions using the TOPSIS method.

Table 4 Results of case-8 of 33 bus system for different weights

Weights	w_p, w_{vd}, w_{vs} (1,0,0)	w_p, w_{vd}, w_{vs} (0,1,0)	w_p, w_{vd}, w_{vs} (0,0,1)	w_p, w_{vd}, w_{vs} (1/2, 0,1/2)	w_p, w_{vd}, w_{vs} (1/3,1/3,1/3)
DG loc's/DG Sizes (KW) /DG pf	13/1095/0.92 24/1169/0.89 30/1405/0.80	13/0938/0.80 23/1983/0.83 30/1408/0.82	12/1144/0.8 23/1870/0.8 30/1331/0.8	13/1109/0.91 24/1204/0.89 30/1395/0.8	**13/1126/0.91 24/1399/0.91 30/1433/0.80**
EVCS loc/EVCS Sizes (KVA)	13/300,30/300 24/150,19/150	13/300,30/300 23/150,19/150	10/300,33/300 23/150,19/150	13/300,30/300 24/150,19/150	**13/300,30/300 24/150,19/150**
RP_{loss} in KW	12.3675	24.649	32.207	12.4194	**13.193**
TVD in p.u	0.0005	0.0002	0.0008	0.0003	**0.00025**
VSI in p.u	0.9697	0.9774	0.9777	0.9747	**0.9756**
% Real power injection by DGs	78.501	93.802	94.14	80.34	**85.76**

D.   IEEE-69 BUS SYSTEM

The single-line diagram of the 69-bus radial distribution system is depicted in Figure 9. A detailed description of the 69-bus system can be found in [12]. The total real and reactive power demand of the system are 3801.4 kW and 2693.6 kVar. The base MVA and kV are 100 and 12.66. In case-0, load flow analysis for the initial assessment of the system without DGs and EVCSs is performed. Load flow results indicate a real power loss of 224.894 kW, TVD of 0.0992 p.u and VSI of 0.6833 p.u.
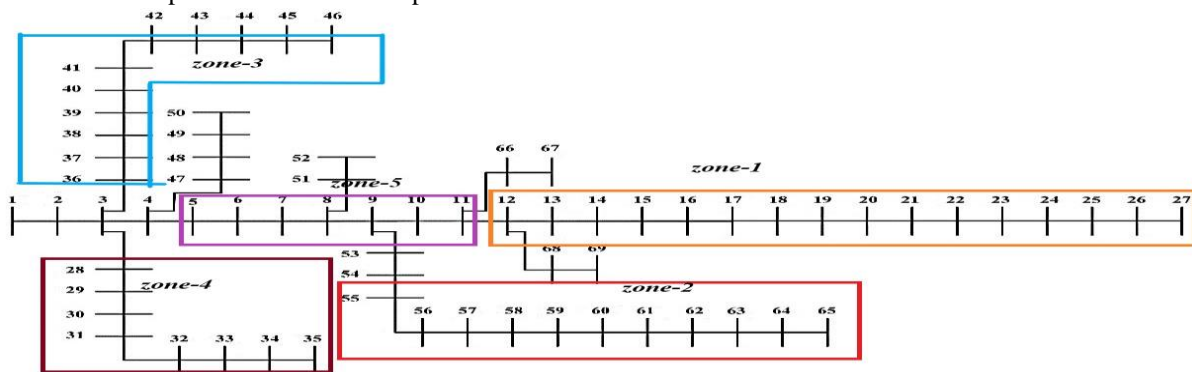
Figure 9 Single diagram of 69 bus system

E.   DGs deployment

Optimal Pareto fronts generated by MOAHO, MOPSO, MOGWO and NSGA-II algorithms for cases 1-4 of the 69-bus system are depicted in Fig 10.
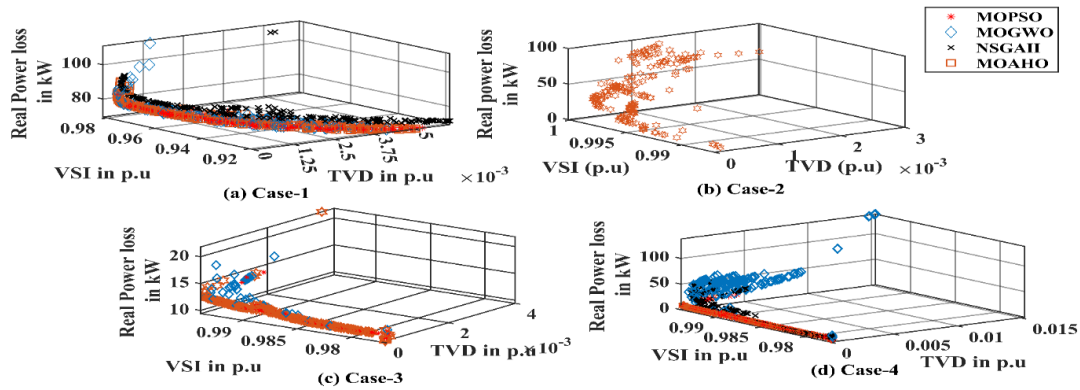
Figure 10 Optimal Pareto fronts of MOAHA, MOPSO, MOGWO & NSGA-II algorithms for cases 1-4 of the 69-bus system

Table 5 gives the optimal locations, DG sizes and DGs pf given by the TOPSIS-MOAHO algorithm for cases 1-4 of the 69-bus system. The utmost improvement in three technical metrics is observed in case-4 during optimal planning of DGs operating with optimal pf i.e., power loss is reduced to 98.053 %, TVD is mitigated to 0.00009, VSI is maximized to 0.9772.

Table 5 Results of 69 bus system for cases 0-4

Case No	DG loc's/DG Sizes (KW/kVAR) /DG's pf	RP_{loss} in KW	TVD in p.u	VSI in p.u	% RP_{loss} reduction	Minimum Voltage in p.u
0	---------	224.894	0.0992	0.6833	----------	0.9092
1	11/0850/120/0425/1 61/2120/1	78.181	0.00025	0.9770	65.253	0.9942
2	11/0471/1,18/0356/1 61/1729/1,21/0478/0 49/1239/0,61/1209/0	6.8742	0.00005	0.9921	96.949	0.9980
3	11/0596/0.9 61/1835/0.9 18/0405/0.9	9.4546	0.00009	0.9772	95.798	0.9943
4	**11/0561/0.80 19/0366/0.85 61/1682/0.81**	**4.3802**	**0.00009**	**0.9772**	**98.053**	**0.9943**

F. Simultaneous DGs & EVCSs deployment

Based on the survey reported in [37], the optimal planning of one charging station in each zone depicted in Figure . 9 with a total of five charging stations having a total charging station capacity of 1100 kVA are considered in the 69-bus system. Optimal Pareto fronts generated by MOAHA, MOPSO, MOGWO and NSGA-II algorithms for cases 7-8 of the 69-bus system are depicted in Figure 11.
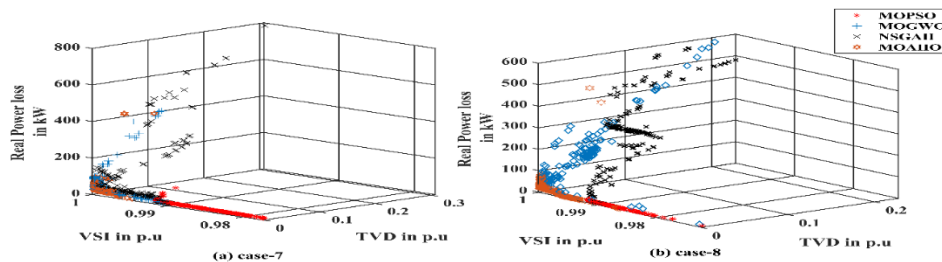
Figure 11 Optimal Pareto fronts of MOAHA, MOPSO, MOGWO & NSGA-II algorithms for cases 7-8 of the 69-bus system

The outcomes like DGs locations, DGs sizes, DGs pf, EVCSs locations, EVCSs sizes, and system technical parameters for cases 5-8 were generated using the TOPSIS-MOAHO algorithm (with equal weightage (w_p, w_{vd}, w_{vs})=1/3) are tabulated in Table 6.

Table 6 Results of 69 bus system for cases 5-8

Case No	DG loc's/DG Sizes (KW/KVAR) /DG's pf	EVCS loc/EVCS Sizes (KVA)	RP_{loss} in KW	TVD in p.u	VSI in p.u	% RP_{loss} Reduction	Minimum Voltage in p.u
5	11/0596/0.9 61/1835/0.9 18/0405/0.9	06/150,17/300 39/300,30/150 55/200	14.6417	0.0039	0.938	93.450	0.9841
6	12/0427/1 22/0633/1 61/1936/1 12/0619/0 25/0290/0 61/1186/0	06/150,23/300 39/300,30/150 58/200	7.6310	0.00014	0.9947	96.608	0.9943
7	10/0755/0.9 17/0723/0.9 61/1966/0.9	10/150,17/300 39/300,30/150 58/200	9.5492	0.00012	0.9964	95.755	0.9943
8	**09/1058/0.88 18/0746/0.87 61/1639/0.80**	**07/150,18/300 39/300,30/150 55/200**	**6.1753**	**0.00013**	**0.9929**	**97.255**	**0.9943**

The utmost improvement in three technical metrics is observed in case-8 during simultaneous optimal planning of EVCSs and DGs operating with optimal pf i.e., power loss is reduced to 97.255%, TVD is mitigated to 0.00013, VSI is maximized to 0.9929.

Figure 12 depicts the voltage profile of the system for all the cases 0-8 of the 69-bus system.
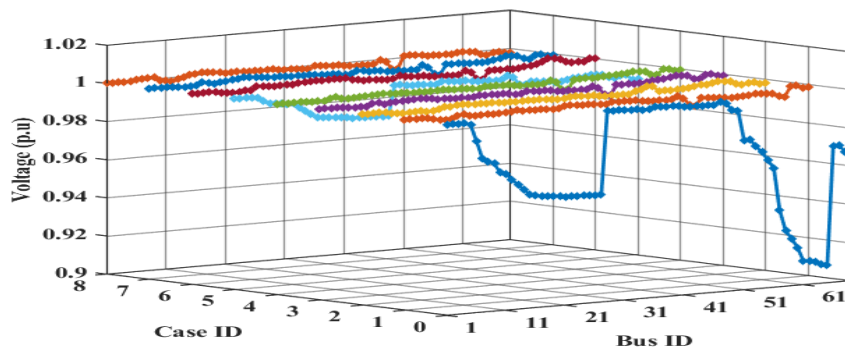
Figure 12 Voltage profile of 69 bus system for the outcomes of TOPSIS-MOAHO with equal weightage generated in different cases

G.   Comparative analysis

Table 07 and 08 depicts the comparison of outcomes generated by the MOAHO algorithm with the MOSPSO, MOGWO & NSGA-II algorithms. From the values quoted in table 07 and 08 it has been observed that the MOAHO algorithm outperforms in all the cases of 33-bus, 69-bus systems. In the proposed optimal planning of the DGs & EVCSs problem, the number of decision variables is 3 in case-1 of the 33-bus & 69-bus system . This shows the effectiveness of the MOAHO algorithm over MOPSO, MOGWO & NSGA2 algorithms over small-size problems having a small number of decision variables to problems having a large number of variables. The

dominance of the MOAHO algorithm over MOSPO, MOGWO & NSGA2 algorithms is also observed from the Pareto fronts depicted in Figures 5,7,10,11.

Table 07 Comparison results of MOAHO with MOPSO, MOGWO & NSGA2 for 33 bus system of cases 1,3,4,7 & 8

Case No	Optimization Technique	DG loc's/DG Sizes (KW)/DG pf	EVCS loc/EVCS Sizes (KVA)	RP_{loss} in kW	TVD in p.u	VSI in p.u
1	**MOAHO**	**13/1155/1, 24/1071/1 30/1572/1**	----------	**91.023**	**0.0012**	**0.9595**
	MOPSO	13/1186/1,24/0943/1 30/1512/1		91.069	0.0016	0.9523
	MOGWO	14/1174/1, 24/975/1 30/1556/1		93.859	0.0013	0.9571
	NSGA2	13/1106/1, 25/806//1 29/1727/1		93.440	0.0015	0.9506
3	**MOAHO**	**13/837/0.9, 24/1177/0.9 30/1350/0.9**	----------	**19.183**	**0.00023**	**0.9768**
	MOPSO	13/835/0.9, 24/1076/0.9 30/1356/0.90		19.249	0.00025	0.9765
	MOGWO	13/839/0.9, 24/1346/0.9 30/1359/0.9		19.895	0.00023	0.9770
	NSGA2	13/863/0.9,24/1123/0.9 30/1264/0.9		18.904	0.00034	0.9764
4	**MOAHO**	**13/810/0.88, 24/1119/0.88 30/1206/0.8**	----------	**13.342**	**0.00024**	**0.9766**
	MOPSO	13/0787/0.86, 24/1052/0.89 30/1204/0.90		13.350	0.00027	0.9763
	MOGWO	12/991/0.9, 24/1033/0.8 30/1162/0.81		15.491	0.00033	0.9768
	NSGA2	13/842/0.89, 24/1029/0.86 30/1175/0.8		13.227	0.00026	0.9764
7	**MOAHO**	**13/1115/0.9, 24/1345/0.9 30/1620/0.9**	**13/300,30/300 24/150,19/150**	**18.142**	**0.00024**	**0.9756**
	MOPSO	13/1090/0.9, 24/1319/0.9 30/1649/0.9	13/300,30/300 24/150,19/150	18.187	0.00026	0.9755
	MOGWO	12/1260/0.9, 24/1211/0.9 30/1654/0.9	12/300,30/300 4/150,19/150	19.738	0.00034	0.9748
	NSGA2	5/2053/0.9, 15/856/0.9 31/1276/0.9	10/300,32/300 24/150,19/150	37.397	0.00080	0.9457
8	**MOAHO**	**13/1126/0.91, 24/1399/0.91 30/1433/0.80**	**13/300,30/300 24/150,19/150**	**13.193**	**0.00025**	**0.9756**
	MOPSO	12/712/0.91, 25/1967/0.82 33/1061/0.93	18/300,33/300 25/150,21/150	23.360	0.00086	0.9599
	MOGWO	10/1385/0.94, 24/1132/0.92 30/1383/0.8	10/300,28/300 23/150,19/150	18.502	0.00054	0.9647
	NSGA2	16/861/0.9, 23/1485/0.9 30/1485/0.8	8/300, 29/300 23/150,20/150	28.505	0.00098	0.9561

Table 08 Comparison results of MOAHO with MOPSO, MOGWO & NSGA2 for 69 bus system of cases 1,3,4,7 & 8

Case No	Optimization Technique	DG loc's/DG Sizes (KW)/DG pf	EVCS loc/EVCS Sizes (KVA)	RP_{loss} in kW	TVD in p.u	VSI in p.u
1	**MOAHO**	**11/850/1,20/425/1 61/2120/1**	-------------	**78.181**	**0.00025**	**0.9770**
	MOPSO	11/807/1,21/436/1 61/2425/1		78.255	0.00026	0.9770
	MOGWO	11/823/1, 21/448/1 61/2139/1		79.366	0.00026	0.9770
	NSGA2	14/952/1,30/28/1 61/2120/1		82.596	0.00025	0.9770
3	**MOAHO**	**11/596/0.9,61/1835/0.9 18/405/0.9**	-------------	**9.4546**	**0.00009**	**0.9772**
	MOPSO	19/455/0.9,61/1846/0.9 66/415/0.9		9.8676	0.00012	0.9772
	MOGWO	15/664/0.9,50/876/0.9 61/1874/0.9		10.591	0.00022	0.9845
	NSGA2	11/563/0.9. 17/405/0.9 61/1832/0.9		9.4845	0.00010	0.9772
4	**MOAHO**	**11/561/0.8, 19/366/0.85 61/1682/0.81**	------------	**4.3802**	**0.00009**	**0.9772**
	MOPSO	18/410/0.8,61/1676/0.81 67/400/0.8		4.7048	0.00012	0.9772
	MOGWO	16/650/0.86,49/674/0.8 61/1774/0.8		6.0106	0.00028	0.9881
	NSGA2	18/559/0.82,50/743/0.8 61/1774/0.81		5.2042	0.00022	0.9824
7	**MOAHO**	**10/755/0.9,17/723/0.9 61/1966/0.9**	**10/150,17/300 39/300,30/150,58/200**	**9.5492**	**0.00012**	**0.9964**
	MOPSO	17/777/0.9,53/866/0.9 61/1824/0.9	07/150,17/300 39/300,30/150,55/200	10.680	0.00018	0.9772
	MOGWO	16/905/0.9,52/426/0.9 61/2000/0.9	06/150,17/300 43/300,32/150,58/200	13.564	0.00034	0.9903
	NSGA2	11/694/0.9, 23/651/0.9 61/2001/0.9	07/150,23/300 43/300,32/150,58/200	17.798	0.00063	0.9915
8	**MOAHO**	**9/1058/0.88,18/746/0.87 61/1639/0.80**	**07/150,18/300 39/300,30/150,55/200**	**6.1753**	**0.00013**	**0.9929**
	MOPSO	16/928/0.89, 49/714/0.8 61/1969/0.83	06/150,17/300 39/300,30/150,55/200	8.048	0.00024	0.9841
	MOGWO	25/600/0.8, 55/771/0.8 61/1579/0.84	07/150,25/300 43/300,30/150,58/200	11.573	0.00106	0.9728
	NSGA2	18/709/0.83,61/1840/0.83 66/598/0.83	10/150,18/300 46/300,32/150,58/200	11.690	0.00071	0.9915

V. CONCLUSION

In this work, the impact on the improvement of distribution system performance under optimal deployment of various DG technologies using the TOPSIS-MOAHO algorithm is presented. IEEE-33,69 bus distribution systems are considered test systems. Enhancement of three technical parameters: real power loss reduction, total voltage deviation minimization and voltage stability index maximization via eight cases is presented in this study. Optimal Pareto fronts for eight cases are generated by the MOAHO algorithm and the most compromised solution is selected using the TOPSIS method. The impact on the objective function's outcomes due to variation of weights

in the TOPSIS method is presented. Maximum enhanced improvement in all the technical metrics has been balanced in all cases during the consideration of equal weightage in the TOPSIS method. Among all the cases, the outmost enhancement improvement in TVD & VSI of the test systems is improved in case-2 i.e., during optimal planning of Type-1 DGs (Micro-turbine etc.) and Type-2 (DSTATCOMs) because injection of active and reactive powers at different buses of the distribution system. Overall balanced improvement in system power loss mitigation, voltage deviation index minimization and voltage stability index maximization are observed during optimal planning of Type-3 DGs operating with optimal pf is observed. Later, simultaneous optimal planning of DGs and EVCSs in the distribution system is presented in the work. The worsening in technical metrics of the distribution system is observed due to the load of EVCS. Optimal planning of DGs and EVCSs has improved the system performance to the above-cited metrics. In terms of achieving the optimal solution, the MOAHO algorithm dominates the MOPSO, MOGWO and NSGA2 algorithms. Optimal planning of DGs and EVCSs considering much more practical insights like load & generation uncertainties, and traffic congestion of PHEVs could be a future scope of work.

REFERENCES

[1] P. Khetrapal, "Distributed generation: A critical review of technologies, grid integration issues, growth drivers and potential benefits," *Int. J. Renew. Energy Dev.*, vol. 9, no. 2, pp. 189–205, 2020.

[2] M. Sedghi, A. Ahmadian, and M. Aliakbar-Golkar, "Assessment of optimization algorithms capability in distribution network planning: Review, comparison and modification techniques," *Renew. Sustain. Energy Rev.*, vol. 66, pp. 415–434, 2016.

[3] G. Pepermans, J. Driesen, D. Haeseldonckx, R. Belmans, and W. D'haeseleer, "Distributed generation: Definition, benefits and issues," *Energy Policy*, vol. 33, no. 6, pp. 787–798, 2005.

[4] A. Ehsan and Q. Yang, "Optimal integration and planning of renewable distributed generation in the power distribution networks: A review of analytical techniques," *Appl. Energy*, vol. 210, no. July 2017, pp. 44–59, 2018.

[5] N. Acharya, P. Mahat, and N. Mithulananthan, "An analytical approach for DG allocation in primary distribution network," *Int. J. Electr. Power Energy Syst.*, vol. 28, no. 10, pp. 669–678, 2006.

[6] D. Q. Hung, N. Mithulananthan, and R. C. Bansal, "Analytical expressions for DG allocation in primary distribution networks," *IEEE Trans. Energy Convers.*, vol. 25, no. 3, pp. 814–820, 2010.

[7] D. Q. Hung, N. Mithulananthan, and K. Y. Lee, "Optimal placement of dispatchable and nondispatchable renewable DG units in distribution networks for minimizing energy loss," *Int. J. Electr. Power Energy Syst.*, vol. 55, pp. 179–186, 2014.

[8] D. Q. Hung, S. Member, N. Mithulananthan, and S. Member, "Determining PV Penetration for Distribution Determining PV Penetration for Distribution Systems With Time-Varying Load Models," *Power Syst. IEEE Trans.*, vol. 29, no. July, pp. 3048–3057, 2016.

[9] P. V. Prasad and S. Satyanarayana, "A Novel Method for Optimal Distributed Generator Placement in Radial Distribution Systems," *Distrib. Gener. Altern. Energy J.*, vol. 26, no. 1, pp. 7–19, 2011.

[10] T. Gözel and M. H. Hocaoglu, "An analytical method for the sizing and siting of distributed generators in radial systems," *Electr. Power Syst. Res.*, vol. 79, no. 6, pp. 912–918, 2009.

[11] A. M. El-Zonkoly, "Optimal placement of multi-distributed generation units including different load models using particle swarm optimization," *Swarm Evol. Comput.*, vol. 1, no. 1, pp. 50–59, 2011.

[12] S. M. and S. K. M. Chandrasekhar Yammani*,†, "Optimal placement and sizing of distributed generations using shuffled bat algorithm with future load enhancement," *Int. Trans. Electr. energy Syst.*, vol. 26, no. April 2015, pp. 274–292, 2016.

[13] S. Kumar Injeti, S. M. Shareef, and T. V. Kumar, "Optimal Allocation of DGs and Capacitor Banks in Radial Distribution Systems," *Distrib. Gener. Altern. Energy J.*, vol. 33, no. 3, pp. 6–34, 2018.

[14] A. Bayat, A. Bagheri, and R. Noroozian, "Optimal siting and sizing of distributed generation accompanied by reconfiguration of distribution networks for maximum loss reduction by using a new UVDA-based heuristic method," *Int. J. Electr. Power Energy Syst.*, vol. 77, pp. 360–371, 2016.

[15] M. M. Aman, G. B. Jasmon, A. H. A. Bakar, and H. Mokhlis, "A new approach for optimum simultaneous multi-DG distributed generation Units placement and sizing based on maximization of system loadability using HPSO (hybrid particle swarm optimization) algorithm," *Energy*, vol. 66, pp. 202–215, 2014.

[16] V. Veeramsetty, C. Venkaiah, and D. M. V. Kumar, *Hybrid genetic dragonfly algorithm based optimal power flow for computing LMP at DG buses for reliability improvement*, vol. 9, no. 3. Springer Berlin Heidelberg, 2018.

[17] A. Parizad, A. H. Khazali, and M. Kalantar, "SITTING AND SIZING OF DISTRIBUTED GENERATION THROUGH HARMONY SEARCH ALGORITHM FOR IMPROVE VOLTAGE PROFILE AND REDUCUCTION OF THD AND LOSSES The Center of Excellence for Power System Automation and Operation , Department of Electrical Engineering , Iran Un," 2010.

[18] S. Arabi Nowdeh *et al.*, "Fuzzy multi-objective placement of renewable energy sources in distribution system with objective of loss reduction and reliability improvement using a novel hybrid method," *Appl. Soft Comput. J.*, vol. 77, pp. 761–779, 2019.

[19] H. Doagou-Mojarrad, G. B. Gharehpetian, H. Rastegar, and J. Olamaei, "Optimal placement and sizing of DG (distributed generation) units in distribution networks by novel hybrid evolutionary algorithm," *Energy*, vol. 54, pp. 129–138, 2013.

[20] S. Sultana and P. K. Roy, "Multi-objective quasi-oppositional teaching learning based optimization for optimal location of distributed generator in radial distribution systems," *Int. J. Electr. Power Energy Syst.*, vol. 63, pp. 534–545, 2014.

[21] V. K. Thunuguntla and S. K. Injeti, "Butterfly optimizer assisted Max–Min based multi-objective approach for optimal connection of DGs and optimal network reconfiguration of distribution networks," *J. Electr. Syst. Inf. Technol.*, vol. 9, no. 1, 2022.

[22] A. Selim, S. Kamel, A. S. Alghamdi, and F. Jurado, "Optimal Placement of DGs in Distribution System Using an Improved Harris Hawks Optimizer Based on Single- And Multi-Objective Approaches," *IEEE Access*, vol. 8, pp. 52815–52829, 2020.

[23] J. Y. Yong, V. K. Ramachandaramurthy, K. M. Tan, and N. Mithulananthan, "A review on the state-of-the-art technologies of electric vehicle, its impacts and prospects," *Renew. Sustain. Energy Rev.*, vol. 49, pp. 365–385, 2015.

[24] S. Mishra *et al.*, "A Comprehensive Review on Developments in Electric Vehicle Charging Station Infrastructure and Present Scenario of India," pp. 1–20, 2021.

[25] F. Ahmad, A. Iqbal, I. Ashraf, M. Marzband, and I. Khan, "Placement of electric vehicle fast charging stations in distribution network considering power loss, land cost, and electric vehicle population," *Energy Sources, Part A Recover. Util. Environ. Eff.*, vol. 44, no. 1, pp. 1693–1709, 2022.

[26] A. Eid, "Allocation of distributed generations in radial distribution systems using adaptive PSO and modified GSA multi-objective optimizations," *Alexandria Eng. J.*, vol. 59, no. 6, pp. 4771–4786, 2020.

[27] S. R. Gampa, K. Jasthi, P. Goli, D. Das, and R. C. Bansal, "Grasshopper optimization algorithm based two stage fuzzy multiobjective approach for optimum sizing and placement of distributed generations, shunt capacitors and electric vehicle charging stations," *J. Energy Storage*, vol. 27, no. December 2019, p. 101117, 2020.

[28] K. E. Adetunji, I. W. Hofsajer, A. M. Abu-Mahfouz, and L. Cheng, "An optimization planning framework for allocating multiple distributed energy resources and electric vehicle charging stations in distribution networks," *Appl. Energy*, vol. 322, no. December 2021, p. 119513, 2022.

[29] Balasubbareddy Mallala, Venkata Prasad Papana, Kowstubha Palle (2023), "Multi-Objective Optimization in the Presence of OGIPFC using NSMMP Algorithm", Recent Advances in Electrical & Electronic Engineering, Vol. 17, Issue 1, pp: 60-81, DOI: 10.2174/2352096516666230504105054

[30] Balasubbareddy Mallala, Divyanshi Dwivedi (2022), "Salp swarm algorithm for solving optimal power flow problem with thyristor-controlled series capacitor", Journal of Electronic Science and Technology, 2022, Volume 20, Issue 2, pp. 1-9. https://doi.org/10.1016/j.jnlest.2022.100156

[31] M Balasubbareddy (2016) "Multi-objective optimization in the presence of ramp-rate limits using non-dominated sorting hybrid fruit fly algorithm", Ain Shams Engineering Journal, Volume 7, Issue 2 pp. 895-905, https://doi.org/10.1016/j.asej.2016.01.005

[32] M Balasubbareddy, S.Sivanaga Raju, Chintalapudi V. Suresh (2015), "Multi-objective optimization in the presence of practical constraints using non-dominated sorting hybrid cuckoo search algorithm", Engineering Science and Technology, an International Journal, Volume 18, Issue 4 pp.603-615,

https://doi.org/10.1016/j.jestch.2015.04.005

[33] M Balasubbareddy, S Sivanaga Raju, Ch Venkata Suresh, AV Naresh Babu, D Srilatha (2017) "A Non-Dominated Sorting Hybrid Cuckoo Search Algorithm for Multi-Objective Optimization in the Presence of FACTS Devices", Russian Electrical Engineering, Volume 88, Issue 1 pp. 44–53, https://doi.org/10.3103/S1068371217010059

[34] Balasubbareddy Mallala, Venkata Prasad Papana, Ravindra Sangu, Kowstubha Palle and Venkata Krishna Reddy Chinthalacheruvu (2022), "Multi-Objective Optimal Power Flow Solution Using a Non-Dominated Sorting Hybrid Fruit Fly-Based Artificial Bee Colony", Energies, 2022, Volume 15, Issue 11 pp. 1-16, https://doi.org/10.3390/en15114063

[35] M. Balasubbareddy, D. Dwivedi, P. V. Prasad (2023), "Optimal power flow solution using HFSS Algorithm", Journal of Electrical and Electronics Engineering Research, Volume 12, Issue 1, March 2023, pp. 1-11, http://www.academicjournals.org/JEEER

[36] N. K. Meena, S. Parashar, A. Swarnkar, N. Gupta, and K. R. Niazi, "Improved Elephant Herding Optimization for Multiobjective der Accommodation in Distribution Systems," *IEEE Trans. Ind. Informatics*, vol. 14, no. 3, pp. 1029–1039, Mar. 2018.

[37] M. M. Sankar and K. Chatterjee, "A posteriori multiobjective approach for techno-economic allocation of PV and BES units in a distribution system hosting PHEVs," *Appl. Energy*, vol. 351, no. September, p. 121851, 2023.

[38] M. M. Sankar and K. Chatterjee, "A posteriori multiobjective techno-economic accommodation of DGs in distribution network using Pareto optimality and TOPSIS approach," *J. Ambient Intell. Humaniz. Comput.*, vol. 14, no. 4, pp. 4099–4114, 2023.

[39] W. Zhao, L. Wang, and S. Mirjalili, "Artificial hummingbird algorithm: A new bio-inspired optimizer with its engineering applications," *Comput. Methods Appl. Mech. Eng.*, vol. 388, p. 114194, 2022.

[40] Kalyanmoy Deb, *Multi-Objective Optimization using Evolutionary Algorithms*. WILEY.

[41] N. Khodadadi, L. Abualigah, E. S. M. El-Kenawy, V. Snasel, and S. Mirjalili, "An Archive-Based Multi-Objective Arithmetic Optimization Algorithm for Solving Industrial Engineering Problems," *IEEE Access*, vol. 10, no. August, pp. 106673–106698, 2022.

[42] P. Phonrattanasak and A. Objectives, "Optimal Placement of DG Using Multiobjective particle Swarm Optimization," *Electr. Technol.*, no. Icmet, pp. 342–346, 2010.

[43] S. Muthukannan and D. Karthikaikannan, "Multiobjective Planning Strategy for the Placement of Electric-Vehicle Charging Stations Using Hybrid Optimization Algorithm," *IEEE Access*, vol. 10, pp. 48088–48101, 2022.

[44] S. Rao, K. Jasthi, P. Goli, D. Das, and R. C. Bansal, "Grasshopper optimization algorithm based two stage fuzzy multiobjective approach for optimum sizing and placement of distributed generations , shunt capacitors and electric vehicle charging stations," *J. Energy Storage*, vol. 27, no. November 2019, p. 101117, 2020.